Journal of Nondestructive Evaluation (2024) 43:108
https://doi.org/10.1007/s10921-024-01122-4

Validation of a Virtual Ray Tracing Instrument for Dimensional X-Ray CT Measurements

Steffen Sloth[1,3] · Danilo Quagliotti[2] · Leonardo De Chiffre[2] · Morten Christensen[3] · Henning Friis Poulsen[1,3]

Received: 31 January 2024 / Accepted: 25 August 2024

Abstract
A new Forward Ray Tracing Instrument (FRTI) for simulating X-ray CT scanners is presented. The FRTI enables the modelling of various detector geometries to optimise instrument designs. The FRTI is demonstrated by comparing experimentally measured sphere centre-to-centre distances from two material measures with digital clones. The measured length deviations were smaller than the reconstructed grid spacing for both the experimental and simulated acquisitions. As expected the experimentally measured length deviations were larger than the simulated measurements. The results demonstrate the FRII's capability of simulating an X-ray CT scanner and performing length measurements.

Keywords X-Ray CT · Metrology · Ray tracing · Monte-Carlo simulation · Aviation security

1 Introduction

Experimental and theoretical modelling of X-ray-instrument design can be performed using a wide selection of stimulation tools, for both research and industry applications. Various tools are used to simulate X-ray Computed Tomography (X-ray CT) instruments, fitting the specific needs of a given research field or industrial application [1–5]. A simulation tool is often optimised to a specific application, such as dose reduction for medical X-ray CT [3–5].

The choice of the simulation tool is often a compromise between simulation time and the image similarity to experimental acquisitions (realism). Simulation tools with short run times, such as Single-Point Ray Tracing [1] or X-ray forward modelling [2], can simulate X-ray CT measurements within seconds to minutes. This is generally achieved by forward projecting geometrical features onto a detector plane. This comes at the cost of reduced realism since only a few X-ray interaction mechanisms are normally modelled, such as photon absorption. Simulation tools modelling the X-ray interaction mechanisms in greater detail can achieve improved realism by utilising e.g. Monte-Carlo based forward ray tracing [6] or wavefront propagation [7]. However, they often suffer from long simulation times. Several new simulation tools are under development trying to overcome these challenges focusing on different research and industrial applications [2, 6, 8].

The development of the next generation of energy dispersive Photon Counting Detectors (PCDs) [9] has sparked new industrial development. The commercial PCDs currently available are still more expensive than scintillator-based detectors and generally only cover a small spatial range. The limited spatial range can be overcome by combining multiple detector modules into an array of PCDs increasing the instrument price and complexity. Modelling the performance

Danilo Quagliotti, Leonardo De Chiffre, Morten Christensen and Henning Friis Poulsen have contributed equally to this work.

✉ Steffen Sloth
stslot@dtu.dk

Danilo Quagliotti
danqua@dtu.dk

Leonardo De Chiffre
ldch@dtu.dk

Morten Christensen
mc@exruptive.com

Henning Friis Poulsen
hfpo@fysik.dtu.dk

[1] Department of Physics, Technical University of Denmark, Fysikvej 1, Kongens Lyngby 2800, Copenhagen, Denmark

[2] Department of Civil and Mechanical Engineering, Technical University of Denmark, Koppels Allé Building 404, Kongens Lyngby 2800, Copenhagen, Denmark

[3] Research and development, Exruptive A/S, Højnæsvej 75, Rødovre 2610, Copenhagen, Denmark

Published online: 21 September 2024

of the gantry's geometry is an important task for optimising the utilisation of the PCDs and reducing the cost.

Among the new industrial designs there is a new type of aviation security scanner utilising PCDs in a fixed-gantry configuration composed of multiple X-ray sources and detector arrays [10]. Fixed-gantry configurations can speed up acquisitions by eliminating the rotating gantry, at the cost of increasing the complexity of the instrument geometry by having multiple sources and detector arrays to manage. Instrument designs using fixed-gantry configurations have been implemented for several research applications [11–13]. However, fixed-gantry instruments have not yet been seen in a large-scale industrial implementation.

Modelling the performance of instruments with a fixed-gantry configuration and estimating the expected data quality is a major challenge, due to the reduced number of imaged projections and increased geometrical complexity of the gantry. A simulation instrument to aid in the modelling and optimising of instrument configurations would benefit future research and industrial developments.

This work presents a new Forward Ray Tracing Instrument (FRTI) to simulate X-ray CT images for modelling the performance of the instruments using fixed-gantry configurations and detector arrays composed of multiple PCD modules. The FRTI is modelled in the well-established Monte Carlo based forward-ray tracing software McXtrace [6]. The paper is organized as follows. The instrument's implementation in the McXtrace framework is described in Sect. 2. Section 2 presents an analysis of the simulated CT acquisition of two material measures (calibrated reference standards according to VIM [14]). From the reconstructed 3D volume a series of sphere centre-to-centre distances are evaluated and compared to their reference lengths. The length deviations evaluated from the simulated data are compared with experimental CT acquisition of the two material measures. Section 4 compares the experimental and simulated results and discusses the future work required to model instruments with a fixed-gantry and array of PCDs.

2 The New McXtrace Simulation Instrument

The new FRTI is modelled using the free and open-source simulation tool McXtrace [6]. McXtrace is a Monte Carlo based forward ray tracing simulation software package. McXtrace can handle energy-dispersive ray tracing, which increases realism and allows for the modelling of energy-dependent instrument properties.

In the McXtrace environment, an instrument is modelled as a consecutive list of X-ray *components*. The list often begins with the source and usually ends with a monitor (detector). During a McXtrace simulation rays are traced sequentially through the list of components. Instead of tracing individual photons, McXtrace traces photon bunches, so-called rays, to increase the simulation efficiency. McXtrace keeps track of the coordinate position ($\mathbf{r} = x,\ y,\ z$), the wavevectors ($\mathbf{k} = k_x,\ k_y,\ k_z$), the phase (phi), the ray energy (E), the weight factor (p), and the simulation run timer (t). A McXtrace component is a self-contained piece of C-code which can modify and record the parameters of a ray. During a simulation, the parameters of each ray are initialised at the source component from a Monte Carlo draw and traced sequentially through the instrument's list of components. A schematic representation of the new FRTI is shown in the centre box of Fig. 1.

The new FRTI is composed of three main components: the X-ray source, the object volume, and the PCD array, seen in the centre box of Fig. 1. The simulated object is provided as a 3D voxel object volume and placed between the source and detector array. The McXtrace component used for the 3D object volume has earlier been demonstrated to perform energy-dispersive simulations of multiple materials [15]. The required input files to run a simulation are shown to the left in Fig. 1 and are as follows:

- An object volume and list of material properties. The object volume is represented as a segmented 3D voxel volume, where each material has a unique integer value, called the material index. Three lists must be provided for each material in the 3D voxel volume. The lists describe each material's energy-dependent Linear Attenuation Coefficient (LAC) and probability of coherent and incoherent scattering. The lists with material properties are generated using the NIST [16] and XCOM [17] databases.
- Two geometry files. The first defines the X-ray source focal position and orientation relative to the instrument's centre of rotation. The second lists the position and orientation of each detector module in the array relative to the source position and orientation.
- A list of operation settings. The settings define the general parameters such as the focal spot size, pixel size, detector energy range, number of detector energy bins, etc. These operation settings can be set as part of the command call or using an input file.

The 3D voxel grid is simulated according to its energy-dispersive interaction mechanisms. Inside the volume a ray is propagated step-wise forward in small increments. In each step, the ray position is used to look up the material index of the voxel which the ray is inside. The material index is used to identify which material properties should be used. The ray's wavevector, energy, and weight factor are adjusted accordingly. Due to limitations in the file formats accepted by McXtrace, the segmented object volume needs to be rep-

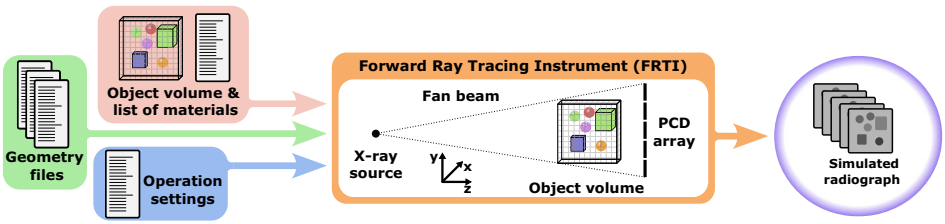

Fig. 1 An overview of the required input files and information on the left to run a simulation. A simplified illustration of a FRTI configuration in the centre box. The rays are traced from the X-ray source through the object volume onto the PCD array where the ray position and energy are recorded. The output is an energy-dispersive radiograph, where the number of energy bins is set using the operation settings

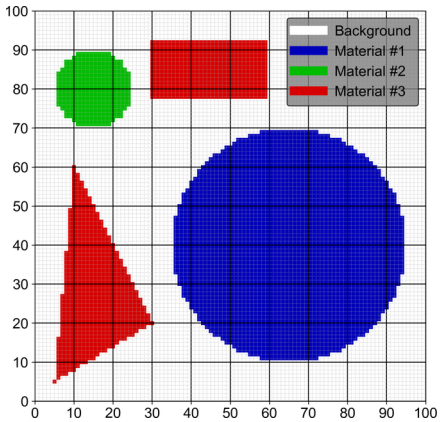

Fig. 2 2D slice of an example of an object volume for the corresponding FRTI's component. The slice contains four separate objects composed of three different materials. All voxels of the same material share the same integer value, called the material index. The material index is used to look up the LAC and scattering probabilities for the given material from the lists of material properties

resented as a stack of slices. Further development is required before other file formats are allowed.

A 2D slice of an example of an object volume (digital clone) is shown in Fig. 2 with four objects of three unique materials. The grid spacing of the object volume can influence the geometric shape of the reconstructed object. Preliminary studies of the sphere centre-to-centre distances evaluated with a centre-of-mass method indicate no noticeable effect when the object's grid spacing is below the voxel size of the reconstruction volume.

In a real instrument, an X-ray source generates a continuous energy spectrum of X-rays, which are then detected by a PCD. McXtrace software subdivides the whole energy spectrum into a number of energy bins (PCD's energy channels), each one simulated by Monte Carlo draws (rays). A large number of simulated rays (roughly 10^8 to 10^9) is required for each energy channel to achieve *sufficient statistics*.

3 Measurement Configurations and Methods

This section establishes the methods for evaluating the geometric accuracy of the new FRTI by comparing experimental and simulated deviations of dimensional measurements. The measured quantities were length deviations of spheres' centre- to-centre distances. The spheres' centre-to-centre distances are evaluated from 3D reconstructions of X-ray CT data acquired experimentally and from FRTI simulations. The length deviations (measurement errors) are calculated by subtracting calibrated tactile reference values and nominal reference values from the experimental and simulated measurements, respectively. The FRTI was configured as an idealised clone of the experimental instrument. The simulations presented here do not include geometric misalignments or external influence factors, such as thermal expansion, mechanical vibrations, etc. The digital clones used for the simulations were generated from the nominal dimensions of the material measures used for the experimental acquisitions.

3.1 The Material Measures and Digital Clones

Two types of material measures were considered: (1) a cylindrical object made of carbon fibre with four ruby spheres (CT Tube) [18] and (2) a carbon fibre plate with a 5 × 5 array of ruby spheres (CT Ball Plate) [19]. The digital clones were designed according to the nominal dimensions of the two material measures and represented in a cubic grid volume with a grid spacing of 0.25 mm. Preliminary investigations indicate no effect on the evaluation of the sphere positions in the simulated data when the object's grid size, here 0.25 mm, was below the grid size of the reconstructed volume (1 mm).

3.1.1 The CT Tube

The CT Tube was designed and manufactured at the Technical University of Denmark (DTU) for system scale correction [18] and had previously been used to demonstrate the dimensional accuracy of the EDXCT [20]. The CT Tube seen in Fig. 3a was made of a carbon fibre tube with a nominal outer

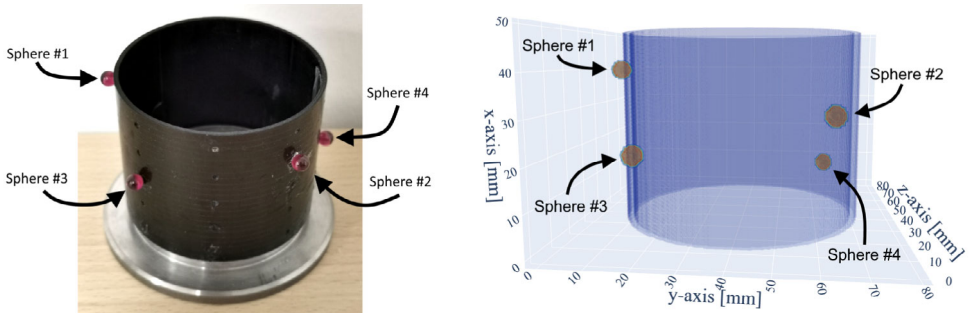

(a) (b)

Fig. 3 A picture of the experimental material measure CT Tube in the left (**a**) and a 3D rendering of the simulated digital CT Tube in the right (**b**). The four spheres were numbered from top to bottom. The coordinate system in **b** was aligned with that of the instrument in Fig. 1

Table 1 List of the six measurands defined as the 3D distance from the centre of spheres indexed N and M

Measurand	Sphere N	Sphere M	Reference sphere centre-to-centre distance	
			Material measure	Digital clone
D1	#1	#2	63.72 mm	63.61 mm
D2	#1	#3	32.90 mm	32.82 mm
D3	#1	#4	69.49 mm	69.62 mm
D4	#2	#3	49.15 mm	49.11 mm
D5	#2	#4	52.23 mm	52.07 mm
D6	#3	#4	68.69 mm	68.73 mm

The sphere numbers indicate which spheres were used for the centre-to-centre evaluation. The spheres' centre-to-centre distances for the material measure were measured using a Zeiss PRISMO CMM with a standard uncertainty $\sigma_{CMM} < 6\,\mu$m. The digital clone was generated based on the nominal dimensions of the material measure

diameter of 63.0 mm and wall thickness of 1.6 mm. Glued to the outer tube wall were four ruby spheres with a nominal diameter of 5.0 mm. The digital clone, shown in Fig. 3b, was generated according to the nominal dimensions in the design of the material measures. The materials chosen for the digital CT Tube's sphere and tube wall were solid carbon and silicon oxide, respectively.

Table 1 lists the six unique sphere centre-to-centre distances. The sphere distances of the experimental differ no more than 0.16 mm from the nominal dimensions of the digital clone.

3.1.2 The CT Ball Plate

The CT Ball Plate seen in Fig. 4a was developed at DTU to evaluate measurement errors in X-ray CT systems [19]. The CT Ball Plate material measure was designed to characterise the probing error of spheres, length measurement error between spheres centres, and volume measurement errors [19]. The 25 ruby spheres have a nominal diameter of 5.0 mm and were fixed to a 2.0 mm thick carbon fibre plate in a square grid with a 10 mm centre-to-centre distance between neighbouring spheres. The digital CT Ball Plate shown in Fig. 4b used for the simulations was generated with the nominal dimensions of material measure in a volume with a grid spacing of 0.25 mm. During the simulations the plate was set as solid carbon and the spheres as solid silicon oxide.

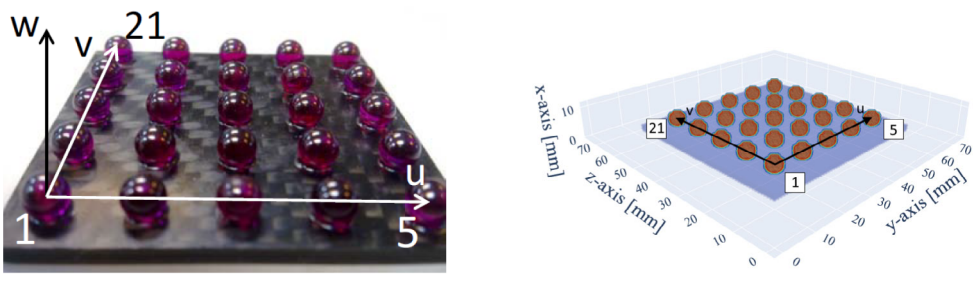

(a) (b)

Fig. 4 A picture of the CT Ball Plate material measure in the left (**a**) and an illustration of the simulation digital clone in the right (**b**). As illustrated, the spheres were numbered row-wise from left to right starting from sphere #1 in the left lower corner

3.2 The Experimental and Simulated Instrument Configurations

The experimental measurements were performed by an energy-dispersive X-ray CT (EDXCT) instrument with a rotating gantry CT scanner [20]. The source and detector positions were based on the mechanical drawings of the experimental instrument and given in Table 2. The source had a tungsten anode target and operated with an acceleration voltage of 160 kV and a current of 5 mA. The focal spot size was 1.6 ×0.8 mm (IEC336). The linear detector array, shown in Fig. 1, was composed of ten ME100 PCDs from the manufacturer Detection Technology [21]. The detectors had 128 × 1 pixel with a pixel size of 0.8 × 0.8 mm and 128 energy bins over an energy range from 20 keV to 160 keV. The object volumes were centred and translated along the axis of rotation (x-axis in Fig. 1) with a transverse grid spacing of 1 mm. The data quality was generally best near the centre of rotation. The 2D projections were reconstructed using an Algebraic Reconstruction Technique (ART) algorithm combined with Total-Variation (TV) minimisation [22]. The input files for the simulation tool were configured to model the EDXCT prototype with the source and detector positions defined in Table 2.

The experimental EDXCT instrument had 10 detector modules stacked vertically. However, with a magnification $m = 1.45$, the magnified shadows of the two material measures and the sample cylinder (used for sample fixture) were just slightly wider than one and five detector module, respectively. The efficiency of the simulations was increased by reducing the field-of-view to only the centre 5 detector modules, listed in Table 2, since the total number of rays thereby could be reduced. The experimental acquisitions were performed with all 10 modules and cropped during the data post-analysis to the five centre detectors. This was not expected to influence the measurement of the sphere positions since the excluded detectors did not image any part of the sample, and of the sample cylinder.

Table 2 List of a source and five detectors' positions from the mechanical drawings of the experimental instrument setup

	Coordinate	
Component	z [mm]	y [mm]
Source	−1018.5	0
Detector #1	478.26	208.00
Detector #2	478.26	104.00
Detector #3	478.26	0.00
Detector #4	478.26	−104.00
Detector #5	478.26	−208.00

These positions were used to define the geometry of the simulated setup gantry and the geometry for the reconstruction algorithm. The coordinates are relative to the centre of rotation of the CT instrument

3.3 The Measurement Procedure

Twenty projections were both experimentally acquired and simulated in each X-ray CT scan with a uniformly spaced rotation of 15°. The simulated and experimental acquired projections were reconstructed using the same ART-TV reconstruction algorithm. The reconstructed volumes had a grid spacing of 1.0 mm in the y, z-plane, while the x-axis' grid spacing is determined by the constant translation speed and the detector integration time. In the experimental acquisitions of the CT Tube and CT Ball Plate the x-axis' grid spacing was 1.0 and 0.8 mm, respectively. In the simulations, the objects were placed in a static position for each line, and in between simulated lines, the object volume was re-positioned linearly along the axis of translation (x-axis of Fig. 1) by a predefined step size of 1 mm.

A total of 10^6 rays were simulated in each line scan. This number of rays was chosen to provide a good contrast between the object and the background while keeping the simulation time within a few hours.

The CT Tube was oriented with the tube's centre axis parallel to the instrument's axis of rotation. The height of the tube could be covered by 65 lines. The average simulation time per line of around 9.5 s with 10^6 rays. The total simulation time for the 65 lines over all 20 projections of the CT Tube was close to 200 min.

The CT Ball plate was orientated with the u,v-plane in the fan beam plane and the w-vector parallel to the direction of translation. In this orientation, twenty simulated line acquisitions were required to cover the height of the CT Ball Plate. The total simulation time with 10^6 rays for all twenty projections was roughly thirty minutes with an average simulation time per line of around 4.1 s. This was twice as fast as for the taller CT Tube since fewer slices need to be loaded compared to the shorter CT Ball Plate.

3.3.1 Evaluating the Dimensional Measurements and Uncertainties

The dimensional measurements were performed from geometrical evaluations of the reconstructed 3D volumes. All the spheres' positions were evaluated from the reconstructed 3D volume using a centre-of-mass (CoM) calculation from a sub-volume near the sphere's expected position. The 3D coordinates evaluated for each sphere's centre position were used to compute the sphere-centre-to-centre distance. The six measurement errors of the CT Tube and the three-hundred measurands of the CT Ball Plate were evaluated from the length deviation between the measured values and corresponding reference values.

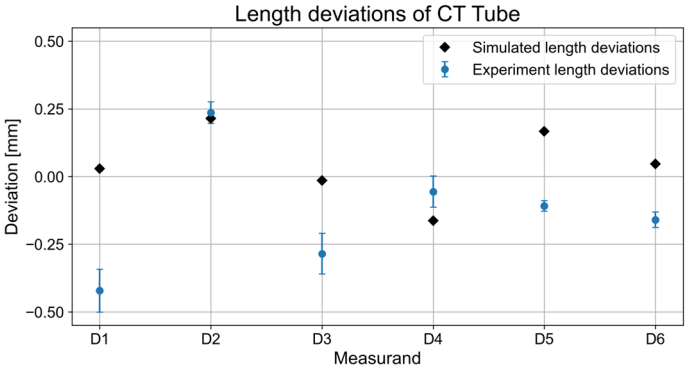

Fig. 5 Length deviation of the six sphere centre-to-centre distances from measurements of the CT Tube from experimental and simulated acquisitions. The error bars for the experimental deviations were evaluated as twice the standard uncertainty ($2\sigma_{CT}$) of the 5 repeated CT acquisitions. The reference length for the simulated data comes from the nominal sphere distances of the digital clone

The experimental reference values were measured using a Zeiss Prismo Coordinate Measuring Machine (CMM). The CMM measurements of the CT Tube and CT Ball Plate were repeated five times with a standard deviation of $\sigma_{CMM} < 6\,\mu m$ and $\sigma_{CMM} < 10\,\mu m$, respectively. The nominal sphere positions were used to calculate the sphere centre-to-centre distances used as the nominal reference values for the simulated measurements.

The experimental uncertainty was evaluated as a type A uncertainty by the standard deviation of measurements from five repeated CT evaluations with a coverage factor $k = 2$ (confidence level of approximately 95 %) [23]. The uncertainty contributions from the CMM measurements were neglected from the combined uncertainty of the CT measurements since it was less than the number of significant digits in the CT measurements.

4 Comparison of Experimental and Simulated Dimensional Measurements

This section presents the length deviations between the sphere centre-to-centre distance evaluated from experimental and simulated CT measurements. The comparison between the two sets of deviations indicated the quality of the FRTI formulation.

4.1 Results Acquired of the CT Tube

The length deviations for the experimental and simulated measurements were within ±0.5 mm and ±0.25 mm of the reference values in Table 1, respectively. The uncertainty of the experimental measurements was evaluated as two times the standard uncertainty of measurements of five repeated CT acquisitions. This was less than the reconstructed volume's grid spacing of 1 mm. No significant trends were observed in the distributions of the six measurands in either the experiments or simulations (Fig. 5).

4.2 Results Acquired of the CT Ball Plate

The 300 sphere centre-to-centre distances for both the experimental and simulated measurements are plotted against the 14 unique nominal lengths in Fig. 6. A linear trend was observed in the deviations for both the experimental and simulated measurements. The slopes of the linear fits were $a_{exp.} = (5.54 \pm 1.13)\,\mu m/mm$ and $a_{sim.} = (2.85 \pm 0.58)\,\mu m/mm$ for the experimental and simulated deviations, respectively. The variations of the two slopes were $\sim 20\,\%$ of the fitted values and from linear regression the coefficient of determination $R^2 \approx 0.27$ for both fits. Therefore, the fits were deemed not satisfactory for the data set's scale correction.

5 Discussion

In this study, we evaluated the geometrical measurement accuracy of the new FRTI using the McXtrace software package. The simulation instrument is evaluated by comparing length measurements from experimental and simulated acquisitions of two material measures: the CT Tube and CT Ball Plate.

The experimental length deviation measurements of the CT Tube are between ±0.5 mm. This is in agreement with earlier studies using the EDXCT instrument [20]. The length deviations from the simulated CT Tube are between ±0.25 mm. For the CT Ball Plate, the standard deviations of the experimental and simulated distributions of length deviations shown in Figs. 6a and 6b were 0.26 mm and 0.12 mm, respectively. The length deviations for both the CT Tube and CT Ball Plate are less than the reconstructed volume's grid size of 1.0 mm for both the experimental and simulated length measurements.

This first work did not consider all the influence factors affecting an energy-dispersive system. Consequently, it is unsurprising that the experimental length deviations for both material measures are larger than the simulated ones. Nevertheless, the implemented formulation of the FRTI, despite

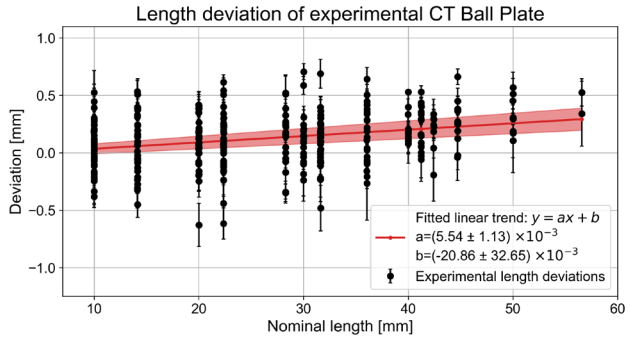

(a)

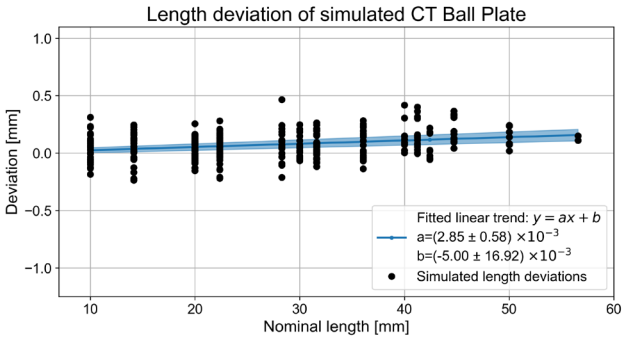

(b)

Fig. 6 Graphs of the CT Ball Plate's sphere centre-to-centre length deviation for the experimental and simulation acquisitions in **a**, **b**, respectively. The 300 centre-to-centre measurements were grouped into 14 unique nominal lengths. The experimental error bars in **a** were evaluated from the standard deviation of 5 repeated measurements on the CT instrument. The parameters and associated uncertainties of the two linear fits were displayed in the legends

not accounting for all the causes of variability, shows a consistent trend with the experimental results and allows for a high level of flexibility and control of the configuration of the simulated X-ray instrument. Therefore, further investigations will follow to model the effects associated with the geometrical misalignment of the gantry and the motion blurring due to the linear translation. In addition, several influence factors will be considered such as non-uniform translation speed, misalignments in the instrument gantry, vibrations during the acquisitions, structure thermal expansion, etc.

A major challenge in developing and testing new material measures using the new FRTI would be the increasing simulation time. The simulation time depends on the size and density of the simulated object volume. This was observed for the simulations of the digital CT Ball Plate being twice as short compared to the digital CT Tube since the voxel volume is half as tall. Working with large voxel volumes would be challenging and future implementations would benefit from a less data heavy data representation of the object volume.

In addition, energy-dispersive simulation using the new FRTI can allow future studies to both investigate the energy-dependent properties of material measures and test digital prototypes of future X-ray CT instrument designs. This capability can offer assistance in modelling the important influence factors for energy-dispersive X-ray CT measurements.

However, the implementation of the energy-dispersive detection is monochromatic requiring the tracing of more rays, which increases the simulation time. An ongoing development of the McXtrace software is aimed at implementing GPU accelerated simulations to reduce the simulation time. For simple McXtrace instruments, GPU parallelisation has already demonstrated upwards of a thousand time reduction in the simulation time [24].

The number of 10^6 rays simulated in the proposed investigation was chosen to provide good contrast in the radiographs between background and object features while keeping the total simulation time short. The contrast in the simulations is expected to be an important contributor to the reduced length deviations observed in the simulation results.

The measurement results demonstrate length deviations of the simulated acquisition of less than half the experimental measurements. Future research should aim at modelling the unaccounted influence factors to produce measurement results more aligned with experimental measurements. Still, more work is needed to model these influence factors. This new FRTI offers great opportunities for such studies by allowing flexible instrument configurations and easy control over the potential influence factors. This could assist in the future development and greater industrial implementation of energy-dispersive X-ray CT instruments.

6 Conclusions

A new FRTI has been presented for simulating X-ray CT instruments. The new FRTI can be used to test and analyse different CT instrument configurations. The FRTI utilises an energy-dispersive McXtrace component to model for energy-dependent absorption and scattering. This enables future development into fully energy-dispersive simulations of X-ray CT instruments utilising PCDs.

The new FRTI was validated by comparing length measurements from CT simulations of digital clones with experimental length measurements of two material measures. A CT Tube and CT Ball Plate were used for comparing the deviation of sphere centre-to-centre distances with experimental and nominal reference lengths. The CT Tube had experimental and simulated deviations within $\pm$ 0.50 mm and $\pm$ 0.25 mm, respectively. The experimental and simulated length deviations of CT Ball Plate were slightly larger at $\pm$ 0.75 mm and $\pm$ 0.50 mm, respectively. All the deviations were below the reconstruction volume's grid spacing of 1 mm. The experimental deviations were around two

times larger than the simulations. This factor of around two is associated with the unaccounted influence factors from geometrical misalignments of the experimental instrument's gantry and motion blurring from the object translation. Further studies are needed to model these influence factors and the FRTI was designed to aid in such investigations.

Future work will consider using the FRTI to evaluate the sensitivity factors of a CT instrument configured with multiple detector modules. Such sensitivity factors are challenging to evaluate experimentally for instruments using detector arrays of multiple modules since it is impractical to measure the position and orientation of all modules. Using the FRTI, geometric misalignments of every instrument's component will be assessed and corrected/compensated.

Acknowledgements This work is supported by the Innovation Fund Denmark (Grant Ref. Number 1044-00087B) and the company Exruptive A/S. The authors would like to thank Klaus Liltorp at DTU Construct for assistance during the CMM measurements of the material measures. The authors would also like to thank Peter K. Willendrup for software support.

Author Contributions The simulations and experiments were performed by SS, together with the data treatment and analysis. All figures and tables were prepared by SS. All authors participated equally in writing the paper.

Funding Open access funding provided by Technical University of Denmark.

Data Availability The simulation tool McXtrace used for the simulation can be downloaded for free on its webpage: https://www.mcxtrace.org/ The specific instrument is in the process of being included as a standard part of McXtrace.

Declarations

Conflict of interest The authors declare no Conflict of interest.

McXtrace software The McXtrace software can be downloaded for free on the McXtrace webpage (https://www.mcxtrace.org/). The new McXtrace instrument is planned to be included as a standard McXtrace instrument for future releases.

References

1. Manerikar, A., Li, F., Kak, A.C.: DEBISim: a simulation pipeline for dual energy CT-based baggage inspection systems. J. Xray Sci. Technol. **29**(2), 259–85 (2021)
2. Autret, A., Fayard, B.: NOVI-SIM: a fast X-ray tomography simulation software for laboratory and synchrotron systems to generate training databases for deep learning applications. In: The 12th Conference on Industrial Computed Tomography, Fürth, Germany (2023)
3. Zaidi, H., Ay, M.R.: Current status and new horizons in Monte Carlo simulation of X-ray CT scanners. Med. Biol. Eng. Comput. **45**, 809–17 (2007)
4. Wu, M., FitzGerald, P., Zhang, J., Segars, W.P., Yu, H., Xu, Y., De Man, B.: XCIST-an open access x-ray/CT simulation toolkit. Phys. Med. Biol. **67**(19), 194002 (2022)
5. Ay, M.R., Zaidi, H.: Development and validation of MCNP4C-based Monte Carlo simulator for fan-and cone-beam x-ray CT. Phys. Med. Biol. **50**(20), 4863 (2005)
6. Bergbäck Knudsen, E., Prodi, A., Baltser, J., Thomsen, M., Kjær Willendrup, P., Sanchez del Rio, M., Ferrero, C., Farhi, E., Haldrup, K., Vickery, A., Feidenhans'l, R.: McXtrace: a Monte Carlo software package for simulating X-ray optics, beamlines and experiments. J. Appl. Crystallogr. **46**(3), 679–96 (2013)
7. Rebuffi, L., Sánchez del Río, M.: ShadowOui: a new visual environment for X-ray optics and synchrotron beamline simulations. J. Synchrotron Radiat. **23**(6), 1357–67 (2016)
8. Bellon, C., Deresch, A., Gollwitzer, C., Jaenisch, G.R.: Radiographic simulator aRTist: version 2. In: 18th World Conference on Nondestructive Testing, pp. 16–20 (2012)
9. Ren, L., Zheng, B., Liu, H.: Tutorial on X-ray photon counting detector characterization. J. Xray Sci. Technol. **26**(1), 1–28 (2018)
10. Sloth, S., Olsen, U.L., Quagliotti, D., De Chiffre, L., Christensen, M., Poulsen, H.F.: Opportunities and challenges of implementing energy dispersive x-ray CT in aviation security screening. E-J. Nondestruct. Test. Ultrason. **28**(3) (2023)
11. Yao, Y., Li, L., Chen, Z.: A novel static CT system: the design of triple planes CT and its multi-energy simulation results. Front. Phys. **7**(9), 632869 (2021)
12. Duan, Y., Cheng, H., Wang, K., Mou, X.: A novel stationary CT scheme based on high-density X-ray sources device. IEEE Access **18**(8), 112910–21 (2020)
13. Zhao, Q., Ma, X., Cuadros, A., Arce, G.R., Chen, R.: Non-linear 3d reconstruction for compressive X-ray tomosynthesis. In: 2020 IEEE International Conference on Image Processing (ICIP), pp. 3149–3153. IEEE (2020)
14. JCGM 200:2012 International vocabulary of metrology—basic and general concepts and associated terms (VIM) joint committee for guides in metrology. Bureau International des Poids et Mesures (BIPM), Sèvres
15. Busi, M., Olsen, U.L., Knudsen, E.B., Frisvad, J.R., Kehres, J., Dreier, E.S., Khalil, M., Haldrup, K.: Simulation tools for scattering corrections in spectrally resolved x-ray computed tomography using McXtrace. Opt. Eng. **57**(3), 037105 (2018)
16. National Institute of Standards and Technology, Standard Reference Database 126: X-Ray Mass Attenuation Coefficients (2022). https://www.nist.gov/pml/x-ray-mass-attenuation-coefficients. Accessed 12 Dec 2023
17. National Institute of Standards and Technology, Standard Reference Database 8 (XGAM): XCOM: photon cross sections database (2022). https://www.nist.gov/pml/xcom-photon-cross-sections-database. Accessed 12 Dec 2022
18. Stolfi, A., De Chiffre, L.: 3D artefact for concurrent scale calibration in computed tomography. CIRP Ann. **65**(1), 499–502 (2016)

19. Müller, P., Hiller, J., Cantatore, A., Tosello, G., De Chiffre, L.: New reference object for metrological performance testing of industrial CT systems. In: 12th Euspen International Conference (2012)
20. Sloth, S., Quagliotti, D., De Chiffre, L., Christensen, M., Poulsen, H.F.: A novel energy resolved X-ray computed tomography instrument for aviation security: preliminary metrological investigation. In: Euspen's 23rd International Conference and Exhibition (pp. 395–398). American Society for Precision Engineering (2023)
21. Detection Technology. https://www.deetee.com/. Accessed 26 Feb 2024
22. Sidky, E.Y., Kao, C.M., Pan, X.: Accurate image reconstruction from few-views and limited-angle data in divergent-beam CT. J. Xray Sci. Technol. **14**(2), 119–39 (2006)
23. JCGM 100:2008 Evaluation of measurement data—guide to the expression of uncertainty in measurement (GUM) Joint Committee for Guides in Metrology. Bureau International des Poids et Mesures (BIPM), Sèvres
24. Knudsen, E.B., Willendrup, P.K., Garde, J., Bertelsen, M.: McXtrace anno 2020-complex sample geometries and GPU acceleration. In: Advances in Computational Methods for X-Ray Optics V, vol. 11493, pp. 46–52. SPIE (2020)